

## Hole Formation in Thin Polymer Films: A Two-Stage Process

Jean-Loup Masson and Peter F. Green

*Texas Materials Institute and Department of Chemical Engineering, The University of Texas at Austin, Austin, Texas 78712*  
(Received 17 May 2001; published 3 May 2002)

Thin, supported liquid films are known to rupture, creating holes throughout the film, due to defects or to van der Waals interactions. We show that the hole formation process before rupturing occurs in two stages, each characterized by distinct dynamical and morphological features. The time scale for the formation process is orders of magnitude slower than the translational (reptation) relaxation time of the individual chains. This has implications regarding the transition from the formation regime to subsequent hole growth regime on the underlying substrate.

DOI: 10.1103/PhysRevLett.88.205504

PACS numbers: 61.41.+e

Structural instabilities, due to destabilizing long-range intermolecular forces, leading to the rupturing of ultrathin polymer films on substrates, have been of interest to researchers during the past decade [1–18]. In addition to scientific reasons, interest in this phenomenon is due to its relevance to the processing of thin films for applications such as polymeric electronic devices, coatings, and patterning (lithographic and nonlithographic).

Theory predicts that three stages characterize the growth of an isolated hole on an underlying substrate [2]. The driving force for growth is due to capillarity. During the first stage, the instability is believed to be rapid in comparison to the translational (reptation) relaxation time,  $\tau$ , of the chains and the radius of the hole,  $R \propto \exp(t/\tau)$  [2]. The second stage occurs when the time scale is sufficiently long that the chains can undergo translational motion and accumulate to form a characteristic rim at the periphery of the hole. In this second stage, if no-slip boundary conditions are valid, the radius increases linearly with time ( $R \propto t$ ) since constant viscous forces balance the capillary driving forces [1,2]. During the third stage, slippage is assumed to dominate and the growth rate decreases because the rim increases in size, thereby increasing the frictional resistance to the capillary driving forces,  $R \propto t^{2/3}$  [2]. A recent paper discusses the implications of slip on hole growth dynamics [19]. We believe that the relative contributions of slip and nonslip boundary conditions should depend on chain length and on chain-substrate interactions.

Despite appreciable experiments and theory on these instabilities [5,6,11,13–20], the hole formation process, prior to rupturing, is not understood. The first studies of dewetting of thin polymer films by Reiter examined the growth of holes on substrates [3,4]. Since then, experiments have concentrated on this growth regime. More recently, simulations by Sharma and co-workers reveal the influence of long and short-range intermolecular forces on the formation of different dewetting, spinodal, or nucleation and growth morphologies as a function of film thickness in homopolymer thin films [13,14]. The nucleation and growth process is dominant in thicker films [6,17,18]. Seeman *et al.* established a very clear experimental connection between the two in the polystyrene/SiO<sub>x</sub>/Si system.

In block copolymer thin films, a new length scale is introduced due to block connectivity. Limary *et al.* showed how the existence of a hierarchy of dewetting morphologies, unique to block copolymer thin films above the bulk ODT, could be reconciled in terms of these interactions [21]. To our best knowledge, apart from these studies, there have been no predictions or experiments regarding the dynamics of the hole formation process.

This Letter examines the morphology and kinetics of hole formation. We show that an initial depression, created by an instability (spontaneous), is initially surrounded by a crest. Two stages, each with distinct dynamical and morphological features, characterize the behavior of this *formation* regime before the depression reaches the substrate (ruptures) where its subsequent *growth* is due to capillarity. The time scale of such an instability is long compared to the translational (reptation) relaxation time of the chains. This has implications regarding the transition between the hole *formation* and *growth* regimes.

The samples were prepared by spin coating a solution of toluene and polystyrene, PS, ( $M_w = 130$  kg/mol) onto silicon substrates which had 2 nm thick native SiO<sub>x</sub> layers, as measured using spectroscopic ellipsometry. Polystyrene films of thicknesses ranging from  $h = 27$  nm to  $h = 102$  nm were investigated in this study. The samples were examined using an autoprobe CP atomic force microscope (AFM), manufactured by Thermomicroscopes in contact mode. Surfaces of the films were observed to be smooth after they were spun. The samples were subsequently annealed for various times at 170 °C in a vacuum oven (the bulk glass transition temperature of PS is 100 °C). Successive images of the samples, quenched to room temperature, were periodically taken of the same regions of the sample each time in order to monitor the change in morphology.

Local depressions, each surrounded by a crest, developed at random locations throughout the surfaces of all films after a few minutes of annealing. Figure 1a shows a typical crest that surrounds a depression in a film of thickness  $h$ , where  $h$  is greater than the depth,  $d(t)$ , of the depression. We characterize each depression by a so-called interfacial angle,  $\theta_d(t)$  and radius  $R(t)$ . The amplitude of a

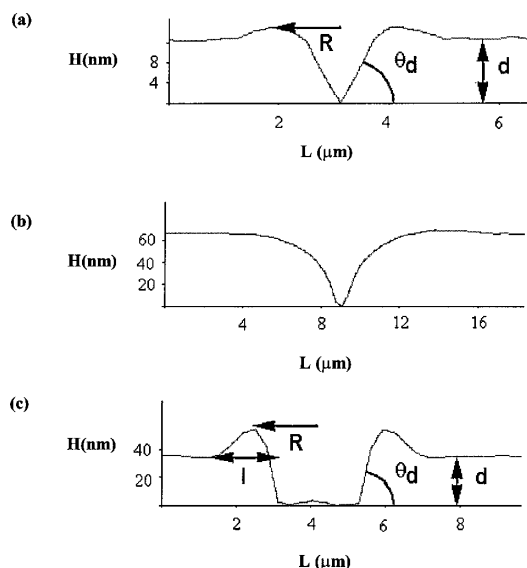


FIG. 1. Characteristics of a hole during the formation stage are shown after 25 min where a crest is located at the perimeter of the hole [part (a)] and after 530 min [part (b)] when the crest has dissipated. The morphology of a typical hole during the growth stage, after the film was ruptured, is shown in part (c).

crest subsequently diminished with time as  $d(t)$  increased (Fig. 1b). The growth regime begins when the depression impinges on the substrate,  $d = h$ , and the characteristic rim of width  $l(t)$  subsequently develops at the perimeter of the hole due to the accumulation of chains (Fig. 1c). Below we show that while the hole formation process is characterized by two stages, three distinct cases, *A*, *B*, and *C*, are possible, depending on film thickness.

The first case is encountered in films thicker than 74 nm. We begin by discussing the radial evolution of a depression in a film of thickness  $h = 102$  nm, Fig. 2. The data in Fig. 2 indicate that formation occurs in two stages. In the first stage, which we identify as FI, the radius grew rapidly with time and after  $t = 35$  min, a transition occurred, denoting the onset of a second stage, FII, where the growth rate of the radius decreased with time. The increase in the depth of the hole,  $d(t)$ , also exhibited two stages;  $d(t)$  initially increased rapidly then subsequently slowed down, abruptly, when it was approximately 3 nm away from the substrate. Even after 3 days at 170 °C, holes in this film did not reach the substrate.  $R(t)$  and  $d(t)$  should have similar time dependencies during the early stage. This is based on the fact that the initial shape of the hole can be approximated by a cone, so  $R \tan(\theta_d) = d$ . Since  $d(t)$  is proportional to  $\exp(t/\tau_d)$  [1,5,16], then  $R = R_0 \exp(t/\tau_d)$ . The lines drawn through the data are consistent with an exponential form. It is noteworthy that the transition from the first formation stage (FI) to the second formation stage (FII) is associated to the dissipation of the crest inside the film. Clearly, each stage is characterized by distinct dynamical and morphological features.

The driving force for the dissipation of the crest into the film is the Laplace pressure. The relaxation time associated with the increase in radius, which reflects the time

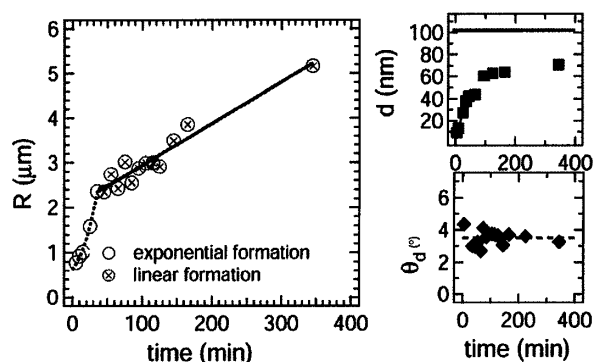


FIG. 2. The two stages of formation are shown here for a hole in a  $h = 102$  nm thick film (case *A*).  $R(t)$ ,  $d(t)$ , and  $\theta_d$  are plotted versus time. In the  $\theta_d$  vs  $t$  graph, the broken line corresponds to the average value of the angle. The error bars in this figure are smaller than the symbols.

associated with dissipation of the crest, is  $\tau_d = 30$  min. This relaxation time might be compared with the longest relaxation time,  $\tau_{\text{rep}}$ , associated with the translational diffusion (reptation) of chains through the polymer melt. For polystyrene chains of this molecular weight,  $M = 130$  kg/mol,  $\tau_{\text{rep}} = 10$  s at the temperature of our experiments [22]. Clearly, the chains move at a rate that is orders of magnitude faster than the time scale that characterizes the dynamics of the instability.

The failure of the hole to reach the substrate is surprising because the disjoining pressure should increase (the distance of the minimum of the hole to the substrate decreases) while the Laplace pressure should remain relatively constant ( $\theta_d$  almost constant). It is plausible that an increasing energetic penalty associated to the creation of a larger surface area of the hole, proportional to  $\pi R(t)d(t)\gamma_{1v}$  (where  $\gamma_{1v}$  is the interfacial energy of the polymer/vacuum interface), may be the reason. Incidentally, this process is expected to be due to heterogeneous nucleation [18].

We now describe a second situation *B*, which would be encountered in films of intermediate thickness  $29 < h < 74$  nm. Here the film is sufficiently thin that the two-stage formation regime and the growth regime are evident. The crest initially forms at the periphery of the hole and subsequently dissipates into the film. The data in Fig. 3 show the transition from the first formation regime (FI) to the slower formation regime (FII) at time  $t = 30$  min. We note that the dissipation of the crest accompanies the transition from the first, FI, to the second formation stage, FII.  $\theta_d(t)$  also undergoes a transition. At time  $t \approx 60$  min the transition from the FII stage to the growth regime occurs when the hole arrives at the substrate. The characteristic rim subsequently develops at the perimeter of the hole and its width  $l(t) \propto t^{1/2}$ , as predicted [1,2]. We note further that during the growth regime,  $dR(t)/dt$  increases whereas  $d(t)$  and  $\theta_d(t)$  become constant, as shown in the inset of Fig. 3.

The second formation stage in case *B* is narrow in comparison to that observed in case *A*. In fact, it should decrease with film thickness. This follows from the fact

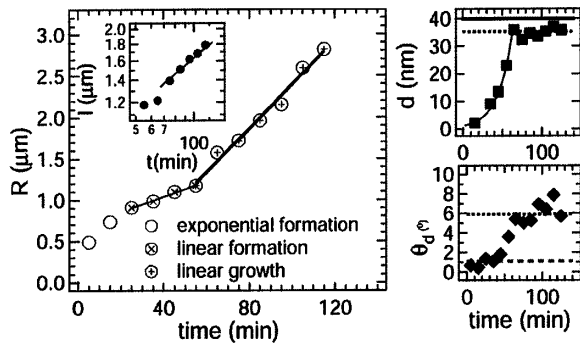


FIG. 3. This figure illustrates the transition from the formation to the growth regime for a film of  $h = 40$  nm at  $t \approx 60$  min when the depression arrives at the substrate. The time dependence of  $R(t)$  increases while  $d(t)$  and  $\theta_d(t)$  become constant in this regime. Further, during this regime  $l(t) \propto t^{1/2}$ . The transition between the formation regimes *FI* and *FII* and the accompanying morphological changes are discussed in the text. (The error bars are smaller than the points.)

that the depression reaches the substrate before the crest has time to dissipate. It follows that in the thinnest films ( $h < 29$  nm), only the first formation stage (*FI*) and the linear growth stage are observed; the second formation stage (*FII*) is bypassed. The dynamics of this third case, *C*, are illustrated in Fig. 4. The onset of the linear growth regime on the substrate that follows the first formation regime (*FI*) is evident from the fact that both  $\theta_d(t)$  and  $d(t)$  [ $d(t) \approx h$ ] become constant and that the width of the rim increases with  $t^{1/2}$ .

We now direct our attention to the transition between the formation and growth stages. When the substrate is exposed, the hole grows because the spreading coefficient of polystyrene on  $\text{Si}/\text{SiO}_x$  is negative. The capillary force, the magnitude of which is proportional to  $|S|$ , is responsible for the increase in the radius of the holes. Since the frictional forces of the substrate/polymer interface, represented by a viscosity at low frequency limit,  $\eta$ , balance the capillary forces [2],

$$R \approx \frac{|S|}{\eta} \left( \frac{b}{h} \right)^{1/2} t. \quad (1)$$

In this equation, the parameter  $b$  is the hydrodynamic extrapolation length that characterizes the slippage of the polymer chains on the substrate.  $b = aN^3/N_e^2$ , where  $a$  is the monomer size,  $N$  is the degree of polymerization of the polymer, and  $N_e$  is the degree of polymerization between entanglements. We reiterate that Eq. (1) is the only growth law that describes our data in the growth regime.

During this linear regime of growth, the rim forms a constant dynamic contact angle,  $\theta_d$ , with the substrate, which, theoretically, differs from  $\theta_e$ , the equilibrium contact angle, by  $\sqrt{2}$ . We measured the dynamic contact angle,  $\theta_d$ , to be  $6^\circ \pm 0.7^\circ$  (Fig. 3), while  $\theta_e = 35^\circ \pm 4^\circ$ . The difference between  $\theta_e/\sqrt{2}$  and  $\theta_d$  can be attributed to contact angle hysteresis of the receding angle [23]. The rim width is predicted to evolve as  $t^{1/2}$  during the linear growth regime, which is observed (Figs. 3 and 4).

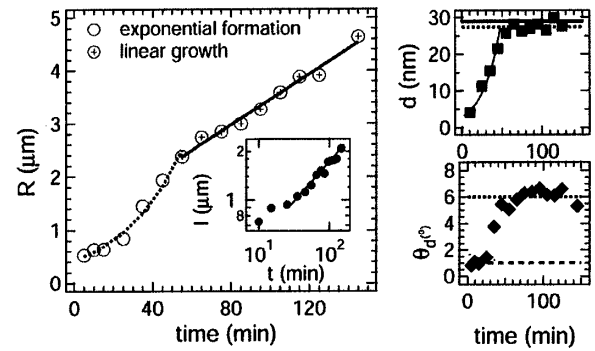


FIG. 4. The (linear) growth regime follows the first (*FI*) formation regime when the film is sufficiently thin,  $h < 29$  nm; the second formation regime is bypassed. In the growth regime  $l(t) \propto t^{1/2}$  while  $d(t)$  and  $\theta_d(t)$  become constant, as expected (insets). (The points are larger than the error bars.)

Equation (1) is theoretically applicable if the extent of the growth of the radius after the substrate is first exposed,  $\Delta R$ , is  $R_{c1} < \Delta R < R_{c2}$ , where  $R_{c1} \sim (bh)^{1/2}$  and  $R_{c2} = b$ . If  $\Delta R < R_{c1}$ , the film is expected to behave like a rubber (instability rate is rapid in comparison to the translational chain dynamics in this entangled system), with the viscous dissipation occurring inside the film. Therefore, in this case, the increase in  $R(t)$  is predicted to be exponential with time and the rim is expected to be absent [2]. In our experiments,  $R_{c1}$  ranges from  $0.71$  to  $1.34 \mu\text{m}$  for films of  $29 < h < 102$  nm. The value of the hydrodynamic extrapolation length for polystyrene of molecular weight  $130$  kg/mol is  $b = 17.5 \mu\text{m}$  ( $a = 3 \times 10^{-4} \mu\text{m}$ ,  $N = 1250$ , and  $N_e = 183$ ) [24]. The range of values of  $R_{c1}$  suggests that this exponential growth should be observed when the substrate is exposed. However, we see no evidence of this. Consider the following explanation. As mentioned earlier, the reptation relaxation time associated with the translational dynamics of the  $M_w = 130$  kg/mol chains is  $\tau_{\text{rep}} = 10$  s at  $170^\circ\text{C}$  [22]. The relaxation time associated with the instability is  $\tau_d = 30$  min, which is orders of magnitude slower. Since  $\tau_{\text{rep}} \ll \tau_d$ , the first exponential growth regime is not expected. Moreover, assuming that  $\tau_d$  is independent of molecular weight, the molecular weight of the polymer would have to be a factor of 6 higher before the first exponential growth stage might be realized in this system,  $\text{PS}/\text{SiO}_x/\text{Si}$ . Therefore, the critical condition defined by  $R_{c1}$  is a necessary, but not sufficient, condition for the existence of the exponential growth regime. Of course, our estimate would be altered if confinement effects influence the transport of the chains. These issues will have to await further experiments and theory. In the siloxane system [25], where the exponential growth regime was observed, the instability was created mechanically and the capillary driving force was comparatively larger. Finally, we note that the power law growth regime is expected when  $\Delta R > b$ , but this is not of interest in this paper.

We presented, for the first time, a complete picture of the formation and growth regimes of an isolated hole created

in a thin polymeric film by a structural instability. Distinct dynamical and morphological features characterize each stage of the formation regime, as in the case for the growth regime. Specifically, a circular crest of radius  $R$  first forms at the periphery of a depression in the film. During this stage (FI), the radius increases exponentially with time,  $R(t) \propto \exp(t/\tau_d)$ , where the relaxation time  $\tau_d$  is large in comparison to the longest relaxation time,  $\tau_{\text{rep}}$ , associated with the translational dynamics of the polymer chains. The crest subsequently dissipates within the film as the depth,  $d$ , of the depression increases and as  $R(t)$  continues to increase. As the crest disappears, a second formation stage (FII) ensues and the growth rate decreases,  $R(t) = \alpha t$ . When the depression impinges on the substrate, the capillary driving forces are responsible for growth,  $S < 0$ . In the first stage of the growth regime,  $R(t)$  also increases linearly with time, but the rate is different from the linear stage of the formation regime.  $R(t) = \beta t$  ( $\alpha \neq \beta$ ) because the viscous forces are balanced by the capillary forces. All the regimes described above would not necessarily be observed in the same film because the process is thickness and molecular weight dependent. If the film is too thick, only the first two formation regimes are observed. If the film is too thin, then the first formation stage occurs. The second formation stage is bypassed in favor of the growth regime.

This work was supported by the National Science Foundation (DMR9705101) and the Robert A. Welch Foundation.

- 
- [1] F. Brochard-Wyart and J. Daillant, *Can. J. Phys.* **68**, 1084 (1991).  
 [2] F. Brochard-Wyart, G. Debrégeas, R. Fondecave, and P. Martin, *Macromolecules* **30**, 1211 (1997).  
 [3] G. Reiter, *Phys. Rev. Lett.* **68**, 75 (1992).

- [4] G. Reiter, *Langmuir* **9**, 1344 (1993).  
 [5] H. S. Khesghi and L. E. Scriven, *Chem. Eng. Sci.* **46**, 519 (1991).  
 [6] K. Jacobs, S. Herminghaus, and K. R. Mecke, *Langmuir* **14**, 965 (1998).  
 [7] R. Segalman and P. F. Green, *Macromolecules* **32**, 801 (1999).  
 [8] R. Limary and P. F. Green, *Langmuir* **15**, 5617 (1999).  
 [9] J-L. Masson and P. F. Green, *J. Chem. Phys.* **112**, 349 (2000).  
 [10] J-L. Masson, R. Limary, and P. F. Green, *J. Chem. Phys.* **114**, 10963 (2001).  
 [11] T. G. Stange, D. F. Evans, and W. A. Hendrickson, *Langmuir* **13**, 4459 (1997).  
 [12] R. Xie, A. Karim, J. F. Douglas, C. C. Han, and R. A. Weiss, *Phys. Rev. Lett.* **81**, 1251 (1998).  
 [13] A. Sharma and R. Khanna, *Phys. Rev. Lett.* **81**, 3463 (1998).  
 [14] R. Konnur, K. Kargupta, and A. Sharma, *Phys. Rev. Lett.* **84**, 931 (2000).  
 [15] J. C. Meredith, A. P. Smith, A. Karim, and E. J. Amis, *Macromolecules* **33**, 9747 (2000).  
 [16] A. Vrij and J. Th. G. Overbeck, *J. Am. Chem. Soc.* **90**, 3074 (1968).  
 [17] R. Seeman, S. Herminghaus, and K. Jacobs, *J. Phys. Condens. Matter* **13**, 4925 (2001).  
 [18] R. Seeman, S. Herminghaus, and K. Jacobs, *Phys. Rev. Lett.* **86**, 5534 (2001).  
 [19] K. Jacobs, R. Seeman, G. Schatz, and S. Herminghaus, *Langmuir* **14**, 4961 (1998).  
 [20] A. J. De Vries, *Rec. Trav. Chim.* **77**, 383 (1958).  
 [21] R. Limary, P. F. Green, and K. Shull, *Eur. Phys. J. E* (to be published).  
 [22] P. F. Green, P. J. Mills, C. J. Palmstrom, J. W. Mayer, and E. J. Kramer, *Phys. Rev. Lett.* **53**, 2145 (1984).  
 [23] M. Morra, E. Occhiello, and F. Garbassi, *Adv. Colloid. Interface Sci.* **32**, 79 (1990).  
 [24] J. Brandrup, E. H. Immergut, and E. A. Grulke, *Polymer Handbook* (Wiley, New York, 1999), 4th ed.  
 [25] G. Debrégeas, P. Martin, and F. Brochard-Wyart, *Phys. Rev. Lett.* **75**, 3886 (1995).